

Design and Development of Control Electronics for Space Rover Hip Yaw Joint Application

Greeshma Chandran¹, Sandip Das², and Dr. Praveen R.P³

¹Assistant Professor, Department of Electrical & Electronics Engineering,
Focus Institute of Science & Technology, Thrissur, Kerala, India.

²Engineer-SD, SRMD/AIS, IISU, Thiruvananthapuram

³Assistant Professor, Department of Electrical Engineering, College of Engineering,
Majmaah University, Saudi Arabia.

³Orcid: 0000-0002-6986-3619

Abstract

The drive system design for a space rover application requires the choice of a motor with high power to weight ratio, low inertia, capacity to develop high acceleration, wide velocity range and high positioning accuracy. Since the control schemes for rover drives are stringent, the system design and control has become an area of wide research. This paper focuses on the development of controller for a precision actuator as per the requirements of space environment. The design utilizes a slotless, coreless PMBLDC motor topology that not only gives high torque to weight ratio and less cogging torque but also limit weight to a few hundred grams. A triangle Pulse Width Modulation technique for Brushless Direct Current (BLDC) motor drives, is proposed based on a comparative study between SVM & SPWM control strategy. The basic drive system design is modeled using Matlab/Simulink environment & is validated with the help of simulation results for confirming the performance characteristics. The results obtained are well within the space requirements which include high torque to inertia ratio, high positioning accuracy, high dynamic response & low detent torque. The hardware implementation of the controller is done using PIC16F877A for speed control of PMBLDC motor actuator.

Keyword– Slotless Brushless DC Motor, Sinusoidal commutation, Space Vector Modulation, Autonomous Rover, Space application.

INTRODUCTION

Space exploration have contributed to all fields of scientific research including medicine, agriculture, defence, technology, predicting natural calamities, forecasting the weather, and communication [1]. Many space missions of NASA, USSR and China are now using robotic systems like Voyagers1 & 2, Mars Pathfinder, and Sojourner etc[2]. Rovers for lunar application place high demands on the system design, control, and performance. The drive system for rover application requires a motor with low inertia, high power to weight ratio, capacity to

develop high acceleration, wide velocity range and high positioning accuracy [5]. Along with above mentioned characteristics drive should also consider the size and weight limitations for space application.

Conventional drive system designs adopted for ground application robots [6-9] cannot satisfy the low size and weight budget for a space exploring robot. Hence the design of a light weight motor and its controller topology that can provide high torque and power efficiency for a space exploring rover is of great research interest. This paper focuses on the design of a drive system meant for an autonomous rover application, considering the requirements of space environment. The drive design selection of Permanent Magnet Brushless DC motor (PMBLDC) and its control electronics for a precise application like an autonomous rover is the main highlight of this work. The paper is organized into two sections, in which section III describes the possibility of selecting a coreless, slotless PMBLDC motor [10,12] with Rhombic winding arrangement for attaining high power and torque density and section V describes the SPWM based control strategy for attaining precise control characteristics. The analysis of controller using Matlab/Simulink model and hardware implementation of the controller using PIC16F877A for speed control of PMBLDC motor actuator are detailed in Sections VI and VII.

NEED FOR ACTUATOR DESIGN FOR AN AUTONOMOUS ROVER

Rovers are space exploration vehicles designed to move across the surface of planets for conducting physical experiments. Mechanical motion of robot is controlled by a closed loop control system. Fig.1 shows the basic schematic representation of a Robotic System meant for space application.

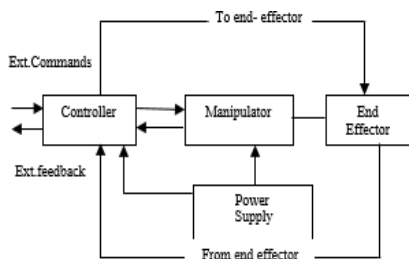


Figure 1: Basic schematic of Robotic System.

The external wireless command and the feedback signal from end effector are compared to obtain reference signal for angular displacement of joint. The reference signal from controller generates motion sequence to the manipulator for the movement of robotic links. The joint movement is utilized by arm, to collect experimental samples for observation which demands for powerful precision actuators with high torque and speed efficiency. But the actuators preferred for ground based robotic applications with high precision have limitations in a space environment, as they do not satisfy the low space and mass budget. The rover actuator design used in this work satisfies the low size & mass requirements along with high torque to inertia ratio, high dynamic response and efficiency. The actuator development including motor and its controller design are described in the following sections.

SELECTION OF ACTUATOR DESIGN FOR AUTONOMOUS ROVER

Brushless DC motors were preferred over Brushed DC motors for electric actuators in rovers as they use electronic commutation techniques and having compact structure. The stator core in conventional BLDC motor, prevents the reduction of overall size of motor [11],[12]. A slotless BLDC motor design on the other hand, has cup shaped winding fixed on the cylindrical stator iron and hence reduce the motor size and weight [15]. The available space can be allotted for permanent magnet, which increases the power density of motor when compared to a slotted one. Airgap windings provide better cooling because the generated heat from windings can be removed not only through the iron but by moving air in the gap. Also ironless motor technology [10],[16],[17],[19] has the advantage of being light weight, compact size, fast acceleration & low cogging torque.

The axial & non-axial winding arrangements are used in electromagnetic actuators used for robots [13],[14]. The axial winding conductors are placed parallel to the motor axis & connected by the endrings. Endrings do not take part in motor torque generation, but it generates joule losses [18,19,22]. Thus to avoid heat losses, Rhombic windings are used [20][21] and the arrangement is represented as in Fig 2.

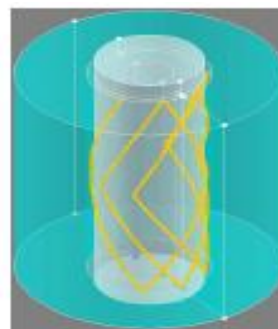


Figure 3: Rhombic winding arrangement [15]

Rhombic windings are utilized for space applications actuators, as they can provide greater utilization of conductors and low iron losses when compared to concentrated windings [24],[25],[27],[28] resulting in high torque to inertia ratio and efficiency. For the purpose of miniaturization of motor, rotor can be equipped with high energy permanent magnets such as Neodymium Iron Boron ($Nd_{20}FeB$) or Samarium-cobalt (Sm_2Co_{17}) magnets. Slotless configuration using Sintered $Nd_{20}FeB$ PM is found to exhibit best performance in terms of power density & torque overload capacity [27]. But $Nd_{20}FeB$ has limitation in space environments as they have poor thermal stability. Based on the advantageous like zero cogging torque, high torque to weight ratio, low inertia, high efficiency, more cooling effect for windings and reduced size slotless, coreless BLDC is identified to be an ideal choice for rover application. Such a motor design within the dimensional requirements of space application actuator is taken to be as shown in Table I.

TABLE I: MOTOR PARAMETERS

| | |
|------------------------------------|----------------------|
| BLDCM Model | 4pole /EC motor |
| Nominal Voltage | 24V |
| Nominal Speed | 14700 rpm |
| Nominal Torque | 53.5 mNm |
| Terminal Resistance phase to phase | 0.527 Ω |
| Terminal Inductance phase to phase | 0.0503 mH |
| Mechanical time constant | 1.48 ms |
| Torque constant | 14 mNm/A |
| Rotor Inertia | 5.54gcm ² |

A four pole PMBLDC motor with mass of 125gms & 22mm outer diameter is selected for space application. The motor specific parameters (Speed and Torque) are line with load requirements. $Nd_{20}FeB$ PM in the rotor provides high flux

density and power density. The non-axial winding arrangement provides higher thermal stability in the range of -20⁰ C to 100⁰ C and is well suited for space environment. The motor parameters given in Table I is used for deriving transfer function of Permanent Magnet Brushless DC motor (PMBLDCM) and is described in the next section.

MATHEMATICAL MODELING OF ACTUATOR

The actuator is a three phase star connected PMBLDC motor and is fed by a three phase voltage source inverter. The assumptions made to derive the motor transfer function and design of motor control parameters are:

- 1) iron and stray losses are negligible
- 2) The three phase stator winding currents are balanced (i_a + i_b + i_c = 0).

The terms R, L, e, V, and i represents the motor parameters such as armature resistance, inductance, back EMF, terminal voltage and phase currents respectively.

The voltage equation corresponding to three phase windings is shown in matrix form as in [13] as:

$$\begin{bmatrix} V_a \\ V_b \\ V_c \end{bmatrix} = \begin{bmatrix} R & 0 & 0 \\ 0 & R & 0 \\ 0 & 0 & R \end{bmatrix} \begin{bmatrix} i_a \\ i_b \\ i_c \end{bmatrix} + \begin{bmatrix} L & 0 & 0 \\ 0 & L & 0 \\ 0 & 0 & L \end{bmatrix} p \begin{bmatrix} i_a \\ i_b \\ i_c \end{bmatrix} + \begin{bmatrix} e_a \\ e_b \\ e_c \end{bmatrix} \dots (1)$$

The equivalent circuit for a phase winding of BLDCM is represented as in Fig 3.

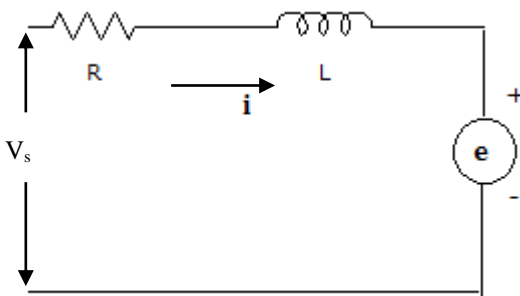


Figure. 3: Per Phase Equivalent circuit of PMBLDCM

Using Kirchhoff's Voltage law the per phase terminal voltage equation under dynamic condition can be written as in [13]:

$$V_s = Ri + L \frac{di}{dt} + e \dots \dots \dots (2)$$

Where V, R, L, i & e represents the per phase terminal voltage, resistance, inductance current & Back EMF respectively.

The electromagnetic torque equation of mechanical system can be modeled using Newton's Second law is given as in [12]:

$$T_e = J \frac{d\omega}{dt} + B\omega + T_l \dots \dots \dots (3)$$

Where, T_e = Electromagnetic torque

J = inertia of load

B= friction constant

T_l= mechanical load torque

The torque constant & back EMF constant equations of motor are:

$$e = K_e * \omega \dots \dots \dots (4)$$

$$T_e = K_t * i \dots \dots \dots (5)$$

From equations (2) & (3),

$$\frac{di}{dt} = -i \frac{R}{L} - \omega \frac{k_e}{L} + \frac{V_s}{L} \dots \dots \dots (6)$$

$$\frac{d\omega}{dt} = -i \frac{K_t}{J} - \frac{B}{J} \omega + \frac{T_l}{J} \dots \dots \dots (7)$$

Taking Laplace transform of equations (6) & (7),

$$sI(s) = -I(s) \frac{R}{L} - \frac{k_e}{L} \omega(s) + \frac{V_s}{Ls} \dots \dots (8)$$

$$s\omega(s) = -I(s) \frac{K_t}{J} - \frac{B}{J} \omega(s) + \frac{T_l}{Js} \dots \dots (9)$$

The transfer function of actuator is the ratio between angular velocity ω, & the source voltage V_s, which is obtained from equation (8) & (9) as:

$$G(s) = \frac{\omega}{V_s} = \frac{1}{\tau_m \tau_e s^2 + \tau_m s + 1} \dots \dots (10)$$

Where τ_m is the mechanical time constant, & τ_e is the electrical time constant

$$\tau_m = \frac{R \cdot J}{K_e \cdot K_t} \quad \dots \dots \dots (11)$$

$$\tau_e = \frac{L}{R} \quad \dots \dots \dots \dots (12)$$

The transfer function, electrical time constant & back EMF constant can be obtained from equations (10), (11) & (12) by substituting motor parameter values from Table I as :

Transfer function of motor, $G(s)$

$$G(s) = \frac{23.657}{(4.708 \cdot 10^{-8})s^2 + (0.00148)s + 1}$$

Electrical time constant, τ_e

$$\tau_e = 0.0318 \text{ ms}$$

Back EMF constant, K_e

$$K_e = 0.04227 \text{ V.s rad}^{-1}$$

The transfer function, electrical time constant & back EMF constant parameters of motor given above can be utilized to model an actuator with high torque to inertia ratio and power density in Matlab/Simulink. Next phase is to develop a controller that can provide high dynamic response to actuator and the design of which is described in the following section.

CONTROLLER DESIGN

The joint movement is controlled by controlling the speed and torque of PMSM. Pulse width modulation is a method for controlling the amount of power delivered to a load without dissipating any wasted power, but by modifying the width of the pulses in a pulse train, in direct proportion to a small control signal; the greater the control voltage, the wider the pulses become [26], [29], [30]. Triangle PWM is a popular voltage PWM scheme that is commonly used to produce a sinusoidal PWM voltage. Application of this scheme to current control is accomplished by making the PWM input as a function of the difference between the desired current and the actual current [31], [32], [33]. Both the turn-ON and turn-OFF of the switch are determined by the intersection of the triangular waveform and the processed current error. The position and

velocity control functionality also allows sophisticated positioning applications.

Mainly two different control types are distinguished for variable frequency drives viz. Scalar control and vector control [34], [35], [36]. In scalar control uses the effect of changing the operating parameters such as voltage and frequency are changed while a vector control dynamically controls the motor's torque directly by observing the motor's current and keeping the magnitude of the instantaneous magnetizing current space vector with reduced torque ripple [37], [38], [39]. It achieves the voltage vector control by adjusting the timing and duty cycle of the eight switching states of the three-phase H-bridge inverter. The eight basic voltage vectors $V_0 \sim V_7$ for a Y-connected motor in the three-phase frame are shown in Fig.4.

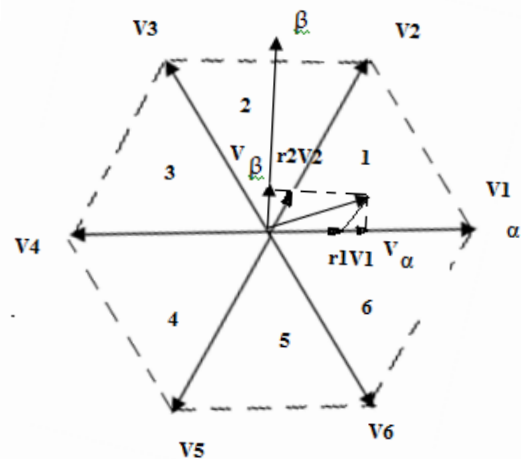


Figure 4: Voltage vectors in the space vector modulation.

Any vectors located in the 6 sectors can be expressed as a linear combination of its nearby basic vectors $V_1 \sim V_6$ and the zero vectors V_0 & V_7 is given as in [5]:

$$v = v_k + r_2 v_{k+1} + \frac{1}{2}(1 - r_1 - r_2)v_0 + \frac{1}{2}(1 - r_1 - r_2)v_7 \quad \dots \dots \dots (13)$$

Where

$$r_1 = \frac{|v| \sin \left[\frac{\pi}{3} - \left(\delta - \frac{k\pi}{3} \right) \right]}{|v_k| \sin \left(\frac{\pi}{3} \right)} \dots \dots \dots (14)$$

$$r_2 = \frac{|v| \sin\left[\left(\delta - \frac{k\pi}{3}\right)\right]}{|v_{k+1}| \sin\left(\frac{\pi}{3}\right)} \dots \dots \dots (15)$$

r_1 & r_2 are the duty cycles & $k=0,1,..,5$ correspond to the sector number. The transistors on/off timing can be calculated as in [5]

$$T_1 = r_1 * T_z \dots \dots \dots (16)$$

$$T_2 = r_2 * T_z \dots \dots \dots (17)$$

$$T_0 = (1 - r_1 - r_2) * T_z \dots \dots \dots (18)$$

where $T_z = 1/f_z$, where f_z is the carrier signal frequency.

A carrier frequency of 50 KHz is used for generating PWM control signals. Space vector control strategy provides higher RMS voltage than with sinusoidal PWM because of the utilization of the 3rd harmonic. Hence the Field Oriented control based algorithm with Sinusoidal current commutation adopted in this paper provides reduced torque ripple and allows precise control and hence can be selected for rover application. The position and velocity control functionality allows sophisticated positioning applications. Figure.5 shows the basic block diagram used for the design of drive system for autonomous rover.

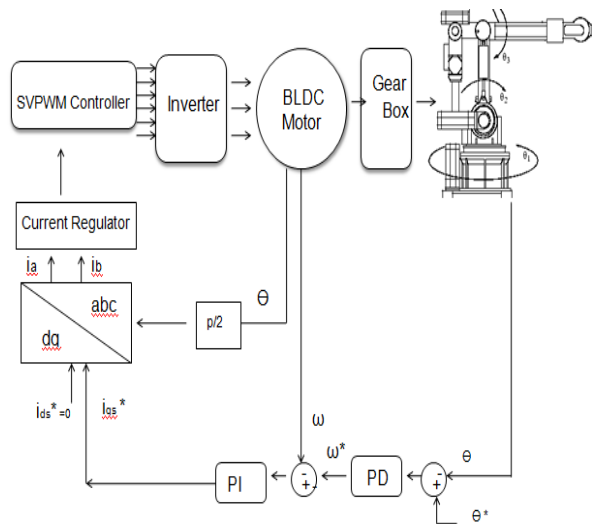


Figure 5: Block diagram of drive system.

The function of the model is to move the joint angle from an initial position to a final angular position. Final angular position is given as a command by the user and is compared with the joint angle feedback from robotic block by position encoders. Error signal is given to Proportional-Derivative controller to generate

speed reference signal ω^* . The speed reference signal is compared with speed feedback from motor (ie. ω) & the error is fed to Proportional Integral controller to generate torque reference T^* . Then T^* is used to generate current reference i_{abc}^* which is given to SVPWM controller block to generate gate pulses for inverter. Torque produced by motor is fed to a speed reducer block & is given to robot block. Speed reducer does the function of a gear system and produce high torque for joint movement. The drive system designed in Matlab/ Simulink environment and the simulation results are presented in the next section.

ANALYSIS OF DRIVE SYSTEM & SIMULATION RESULTS

The basic design of rover is developed as per the requirements of space application and in order to validate the design the drive system has been modeled in Matlab/Simulink environment. The basic Simulink model for the designed joint actuator is shown in Fig. 6. The robotic joint is modeled using the second order equation given as in [5]:

$$T_e = J_i \frac{d^2\theta_i}{dt^2} + B_i \frac{d\theta_i}{dt} + G_i \theta_i \dots \dots \dots (19)$$

Where θ_i is joint angular position, J_i is inertia, C_i is centrifugal and Coriolis coefficient, and G_i is gravitational coefficient.

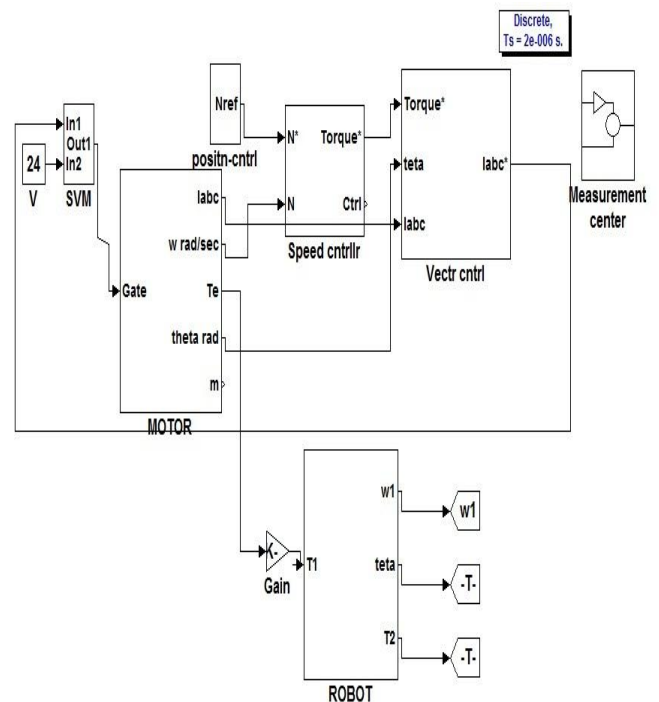


Figure 6: MATLAB/Simulink model of Actuator

The joint is to be moved from an initial angular position θ_{ini} to a final angular position θ_{fin} . In order to validate the performance characteristics of drive system, angular position of joint is varied. Initially the angular position was -30° and is displaced to a new position of 30° which is fed to the position control block as input. The error signals from the comparators are fed to controllers block to generate reference signals. The joint angular displacement and Speed waveforms of robotic joint using SVM and SPWM control strategies are shown in Fig.7, Fig.8.

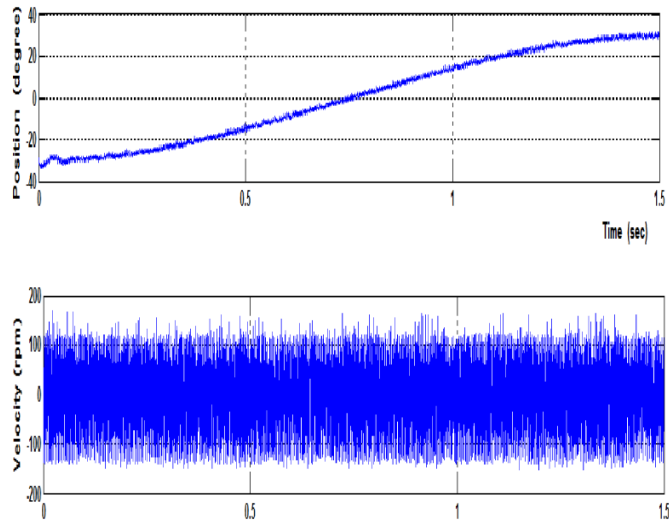


Figure 7: Angular displacement & Velocity waveforms of Robotic joint using SVM control.

The joint angular position is at -30° at time $t = 0$ seconds. The speed is accelerated such that at time $t = 0.9$ seconds joint is displaced to a new position of 30° . As the joint angular position changes the speed reverses and torque value changes from positive to negative. After 0.9 seconds the joint have a tendency to move forward due to inertia which can be avoided by providing a braking torque. The THD analysis of inverter current waveform of PWM and SVM control method is shown in Fig 9(a) and Fig 9(b) below.

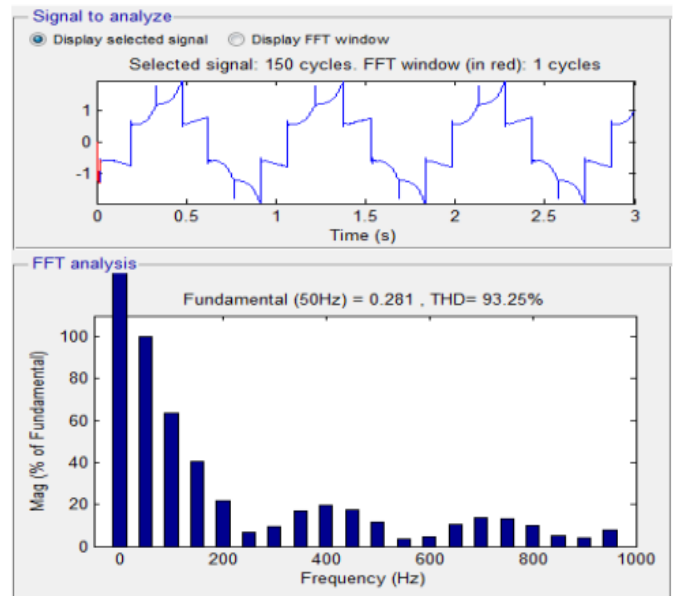


Figure 9(a): THD analysis of Line Current (PWM).

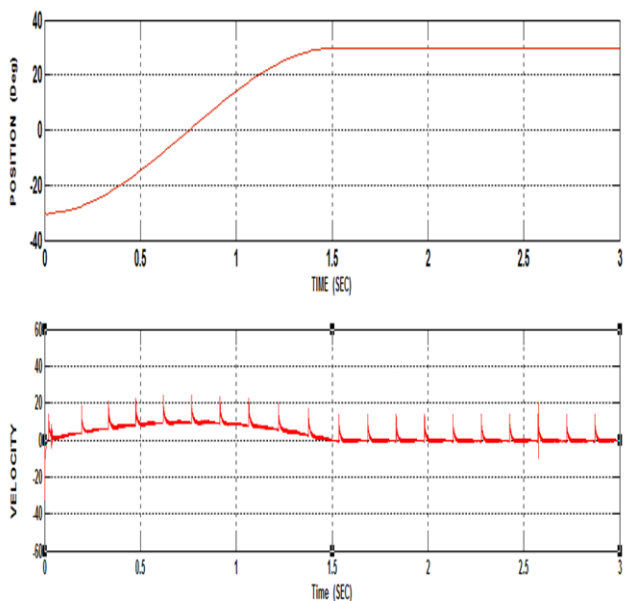


Figure 8: Angular displacement & Velocity waveforms of Robotic joint using SPWM control.

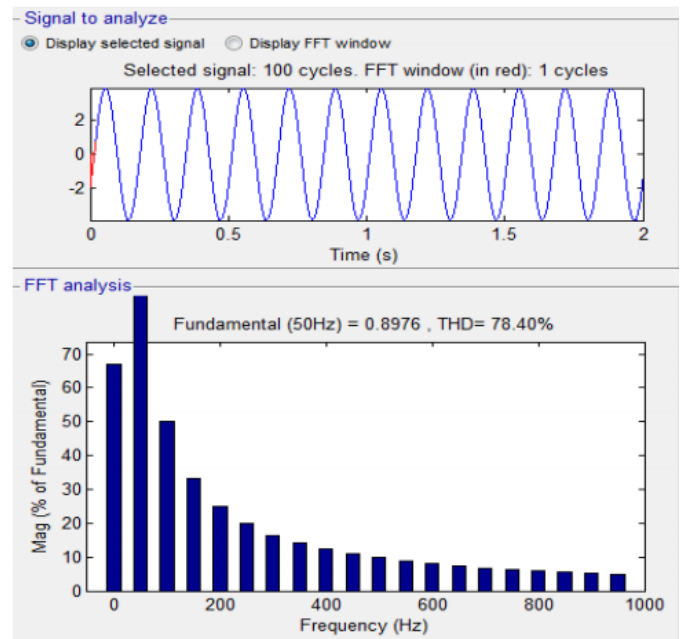


Figure 9(b): THD analysis of Line Current (SVM).

The comparison of THD analysis given in Fig 9(a) and 9(b) shows that SVM control method have lower THD when compared to PWM control method. But low THD can only be attained when torque ripple is high using BLDC- Sinusoidal combination [40],[41],[42],[43],[51]. A comparison of torque ripple in PWM and SVM control methods are also done to find the best control scheme suited for Hip Yaw joint position application.

The waveforms shown in Fig 10(a). and Fig 10(b). given below is used to compare torque ripple in PWM and SVM control methods.

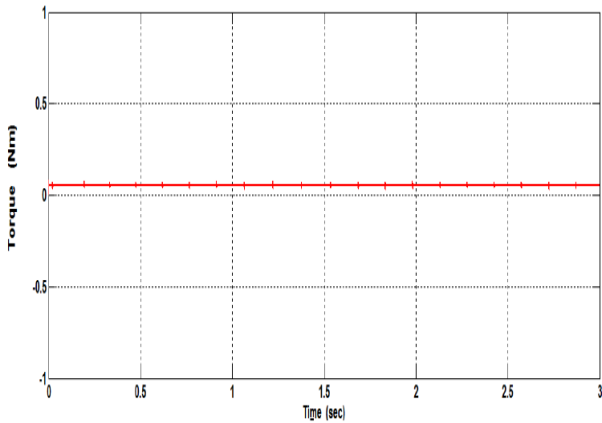


Figure 10(a): Torque waveform at rover joint using PWM control method.

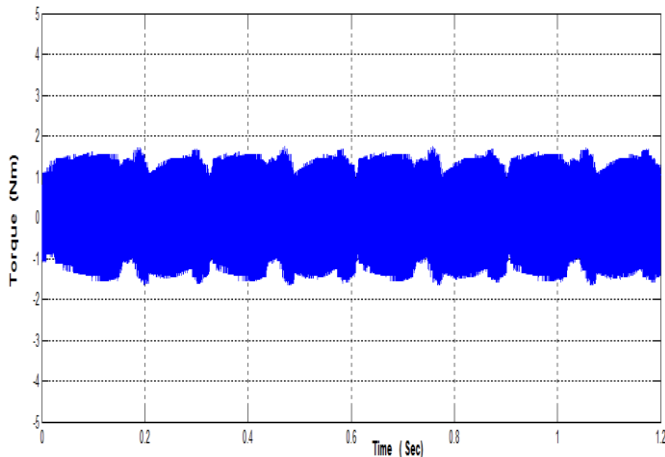


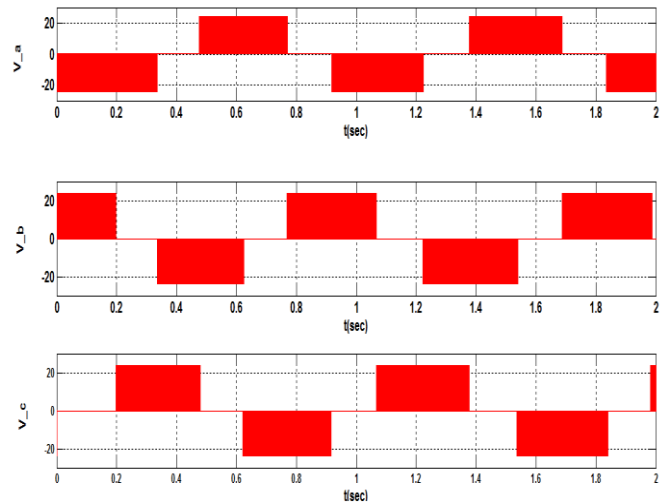
Figure 10(b): Torque waveform at rover joint using SVM control method.

The torque ripple in electrical machines is caused by many factors such as cogging torque, the interaction between the MMF and the airgap flux harmonics, or mechanical imbalances, e.g. eccentricity of the rotor[44],[45],[46][49]. The Maxon 323218 motor has the advantage of zero detent torque and hence

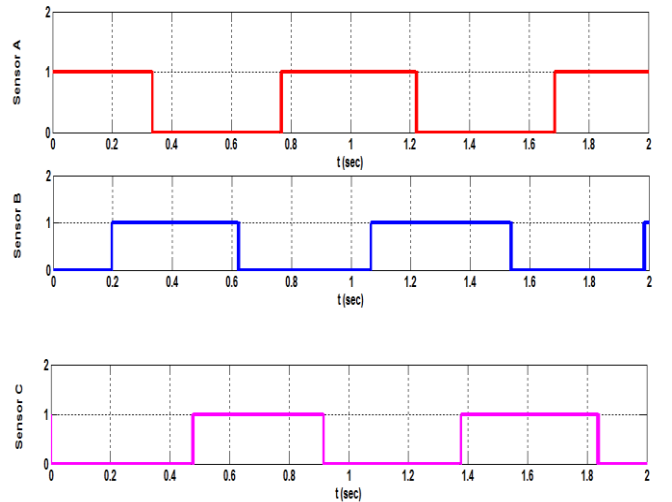
torque ripple can be caused by the control method used. The torque ripple is defined as the percentage of the difference between the maximum torque and the minimum torque compared to the average torque[47],[48],[50],[52]. In PWM control method torque ripple obtained was 12.37% and using SVM torque ripple was 56.074%. For Hip Yaw joint position control of an autonomous rover, Torque ripple reduction is an important factor and hence PWM control method is best suited for Hip Yaw joint position control.

The relationship between the sensor outputs and the required motor drive voltages is shown in Fig 11(a) and 11(b). The inverter switches are triggered and the windings are

energized in sequence with the Hall sensor output signals. The conduction mode of inverter is attained with MOSFET switches with two switches conducting in a conduction interval.



(a)



(b)

Figure 11(a): Motor drive voltage and 11(b) Hall sensor signals waveform.

The simulation results verify that the rover drive system with slotless, coreless motor design with rhombic winding topology provides high torque and power density when compared to SVPWM control method. Pulse Width Modulation control also helps to attain precise control and smooth performance. The hardware implementation of drive system using PWM control strategy is detailed in next section.

EXPERIMENTAL VALIDATION OF DRIVE SYSTEM

The motor drive part consists of Power driver circuit and the Inverter, while Controller part consists of PIC16F877A microcontroller which generates the logic signals. The logic signals are given to driver circuit for amplification and the control signals obtained are transmitted to the MOSFETs, in proper synchronism after providing electrical isolation of control circuit from power circuit. The motor is connected to inverter so that three phase AC output voltage from a constant DC voltage is fed by the inverter to motor. The hardware setup consisting of Drive part, controller part and motor is given in Fig 12 below.

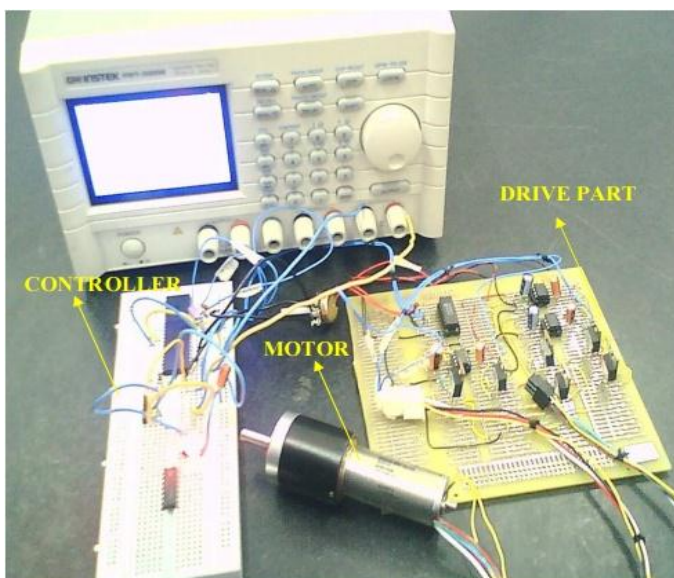


Figure 12: Hardware setup

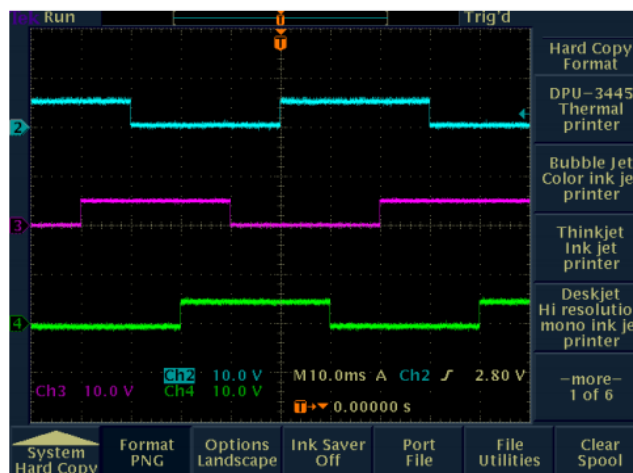


Figure 13: Hall Sensor Signals.

Each sensor element outputs a digital high level for 180 electrical degrees of electrical rotation, and a low level for the other 180 electrical degrees. The three sensors are offset from each other and the period of hall sensor signals are 60ms corresponding to 1000rpm as is in Fig.13. The hardware implementation of position control functionality will be included in the future works.

CONCLUSION

This work aims at development of control electronics for PMBLDC drive system for the movement of hip Yaw joint of a space rover. The selection of slotless, ironless PMBLDC motor design helped in achieving high power and torque density with zero detent torque. Also rhombic winding arrangement helps to limit motor weight to a few hundred grams. The Triangle Pulse Width Modulation offers the possibility to drive brushless DC motors with minimal torque ripple and low noise. Position control of Hip Yaw joint is attained with a low torque ripple of 12.37% which is acceptable for positioning application in space. MATLAB/Simulink results verify that PWM control strategy with position and velocity control functionality allows accurate positioning applications. The hardware implementation of the controller with the specifications is done using PIC16F877A for speed control of PMBLDC motor actuator. The design selection of Permanent Magnet Brushless DC motor and its control electronics for a precise application like an autonomous rover is the main highlight of this work.

ACKNOWLEDGMENT

The authors would like to thank ISRO Inertial Systems Unit, Department of Space, Government of India for their support to carry out this research work.

REFERENCES

- [1] Rob Ambrose, Brian Wilcox, NASA. "DRAFT Robotics, Tele-Robotics and Autonomous Systems Road map Technology Area 04, NASA" Nov 2010.
- [2] Von Sebastian Bartsch "Development, Control, and Empirical Evaluation of the Six-Legged Robot Space Climber Designed for Extraterrestrial Crater Exploration" Dissertation. www.isro.org
- [3] S K Saha, "Introduction to robotics", ISBN-13: 978-0070140011, McGraw-Hill Education, Oct 2008.
- [4] Joo Han Kim, Se Hyun Rhyu, In Soung Jung, Jung Moo Seo "An investigation on the development of precision actuator for small robot" International Conference On Mechatronics And Automation 2009, pp.1049-1053.
- [5] G.Chandran, Das S, Praveen.R.P "PWM based control electronics of a PMLDLC motor for hip yaw joint of a space rover application" Emerging Research Areas: Magnetics, Machines and Drives (AICERA/iCMMD), 2014 Annual International Conference on Year: 2014 Pp: 1 – 6.
- [6] In-Soung Jung, Jung-Moo Seo, Joo-Han Kim, and Se-Hyun Rhyu, "Development of Slotless Type Brushless DC Motors and Planetary Gear Heads for Robot", 9th International Conference on Ubiquitous Robots and Ambient Intelligent 2012, pp.445-448.
- [7] C.C. Hwang, P.L. Li, C.T. Liu, C. Chen, "Design and analysis of a brushless DC motor for applications in robotics", www.ietdl.org
- [8] Jung-Moo Seo¹, Young-Kyun Kim, Se-Hyun Rhyu, In-Soung Jung, and Hyun-Kyo Jung, "A Design of Slotless BLDC Motor for Robot Using Equivalent Magnetic Circuit Model", 8th International Conference on Ubiquitous Robots and Ambient Intelligence, Nov.2011, pp.719-723.
- [9] Yong-Ho Yoo, Mohammed Ahmed, Malte Roemmermann and Frank Kirchner "A Simulation-Based Design of Extraterrestrial Six-Legged Robot System", 35th Annual Conference of IEEE Industrial Electronics, Nov. 2009, pp.2181-2186.
- [10] "Selection of Electric Motors for Aerospace Applications," NASA Document on Preferred Reliability Practices, Practice No. PD-ED-1229, pp.1-6.
- [11] Dr. Otto Stemme, Peter Wolf, - Principles and Properties of Highly Dynamic DC Miniature Motors - Interelectric AG, CH-6072 Sachsen / Switzerland 1994
- [12] Kais Atallah, Z Q Zhu, David Howe, & Terry S. Birch "Armature Reaction Field and Winding Inductances of Slotless Permanent-Magnet Brushless Machines", IEEE Transactions on Magnetics, Sept 1998, Vol. 34, No. 5.
- [13] Y S Chen, Z Q Zhu, D Howe "Slotless Brushless Permanent Magnet Machines: Influence of Design Parameters" IEEE Transactions on Energy Conversion, Sept 1999, vol.14, No.3.
- [14] Nicola Bianchi, Silverio Bolognani, Fabio Luke, "High Speed Drive Using a Slotless PM Motor", 35th Annual IEEE Power Electronics Specialists Conference, June 2004, pp.458-463.
- [15] Miroslav Markovic, Yves Perriard, "Simplified Design Methodology for a Slotless Brushless DC Motor", IEEE Transactions on Magnetics, Dec 2006, Vol. 42, No. 12.
- [16] Praveen R P, Ravichandran, M.H. Achari, V.T.S. Raj, V.P.J. Madhu, G. Bindu, G.R. "A Novel Slotless PMLDLC motor for precise positioning application", IEEE International Conference on Communication Control and Computing Technologies (ICCCCT), Oct 2010, pp. 250 - 254.
- [17] Jung-Moo Seo, Joo-Han Kim, In-Soung Jung, "Design and Analysis of Slotless Brushless DC Motor" IEEE Transactions on Industry applications, March/April 2011, vol. 47, no. 2.
- [18] Andreas Looser, Thomas Baumgartner, Johann W. Kolar, Christof Zwyssig "Analysis and Measurement of Three-Dimensional Torque and Forces for Slotless Permanent-Magnet Motors" IEEE Transactions on Industry Applications, July/August 2012, Vol. 48, No. 4.
- [19] R. P. Praveen, M. H. Ravichandran, V. T. Sadasivan Achari, V. P. Jagathy Raj, G. Madhu, G. R. Bindu "A Novel Slotless Halbach-Array Permanent-Magnet Brushless DC Motor for Spacecraft Applications" IEEE Transactions on Industrial Electronics 2012, pp. 3553 – 3560.
- [20] Greeshma Chandran, Sandip Das, R. P. Praveen "Development of control electronics of a PMLDLC motor for an autonomous rover application in space" International Conference on Circuit, Power and Computing Technologies (ICCPCT), 2014, pp. 280 – 286.
- [21] Kanwar Pal, Saurabh Shukla, Sanjeev Singh "Single current sensor PMLDLC motor drive with power quality controller for variable speed variable torque applications" International Conference on Electrical Engineering and Informatics (ICEEI), 2015, pp.546 – 551.
- [22] S. W. Khubalkar, A. S. Chopade, A. S. Junghare, M. V. Aware "Design and tuning of fractional order PID controller for speed control of permanent magnet brushless DC motor", IEEE First International Conference on Control, Measurement and Instrumentation (CMI) 2016, pp. 326 – 320.
- [23] Muhammed Fasil; Nenad Mijatovic; Bogi Bech Jensen;

- Joachim Holboll "Performance Variation of Ferrite Magnet PMSM Motor With Temperature" IEEE Transactions on Magnetics 2015, vol. 51, Issue: 12.
- [24] A A Aboulnaga & A Emadi "Design of High Performance Linear Brushless DC Motor with Ironless Core" 4th International Power Electronics and Motion Control Conference, IPEMC ,Aug 2004,pp. 502 - 507.
- [25] B. Dehez, M. Markovic and Y. Perriard, "Analysis of BLDC motor with zigzag and rhombic winding", 19th International Conference on Electrical Machines (ICEM), September 2010.
- [26] Bruno Dehez, Miroslav Markovic, and Yves Perriard "Analysis and Comparison of Classical and Flex-PCB Slotless Windings in BLDC Motors", 15th International Conference on Electrical Machines and Systems, Oct 2012, pp.1-6.
- [27] H. M. Cheshmehbeigi ,E. Afjei "Design Optimization of a Homopolar Salient-Pole Brushless DC Machine: Analysis, Simulation, and Experimental Tests" IEEE Transactions On Energy Conversion, June 2013, Vol. 28, No. 2.
- [28] R P Praveen , Ravichandran, M.H.,Achari, V.T.S, Raj, V.P.J, Madhu, G, Bindu, G.R, Dubas, F. "Optimal design of a surface mounted permanent magnet BLDC motor for spacecraft applications", International Conference on Emerging Trends in Electrical and Computer Technology (ICETECT), March 2011 ,pp. 413 – 419.
- [29] K W Lim, M F Rahman, K S Low, L K Chew "Evaluation of software Controllers for permanent magnet Synchronous motor bldc drive" 42nd Southeastern Symposium on System Theory ,March 2010,pp.302-306 .
- [30] S K Safi, P P Acarnley, A G Jack "Analysis and simulation of the high speed torque performance of brushless DC motor drives" IEEE Proc.Electr.Power, ,May 1995, Appl.Vol 142, No.3.
- [31] R. Krishnan and P. Vijayraghavan. "A New power converter topology for PM brushless dc motor Drives" 24th Annual Conference of the IEEE Industrial Electronics Society, Aug-Sep 1998, pp.709-714, vol.2.
- [32] R. Krishnan "A novel single-switch-per-phase converter Topology for four-quadrant PM Brushless DC motor drive", 31st IEEE Industrial Application Conference , Oct 1996, pp.311-318, vol.1.
- [33] Z Q Zhu, S Bentouati, and d Howe "Contol of single phase permanent magnet Brushless DC drives for high speed applications", power Electronics and variable speed Drives , Sept 2000, pp18-19.
- [34] Byoung- Kuk Lee, Mehrdad Ehsani, "A simplified functional simulation model for three- phase Voltage source inverter using switching function concept" IEEE Trans. Ind.Electron., April 2001, ,vol.48,no.2.
- [35] Pragasen Pillay, Ramu Krishnan (1989) "Modeling, Simulation, and Analysis of Permanent-Magnet Motor Drives, Part II: The Brushless DC Motor Drive". IEEE Transactions on Industry Applications Vol: 25, No-2
- [36] Kamran Tabarraee, Jaishankar Iyer, Hamid Atighechi, Juri Jatskevich "Dynamic Average-Value Modeling of 120° VSI-Commutated Brushless DC Motors With Trapezoidal Back EMF" IEEE Transactions On Energy Conversion, , June 2012, Vol. 27, No. 2.
- [37] Vinatha U, Dr.K.P.Vittal, Swetha Pola, "Simulation of Four Quadrant Operation & Speed Control of BLDC Motor on MATLAB / SIMULINK" in Proc. of IEEE Region 10 conference, TENCON, Hyderabad, 2008
- [38] L. Tang and M. F. Rahman, "A Matlab/Simulink Model Based on Power System Blockset-A New Direct Torque Control Strategy for Interior Permanent Magnet Synchronous Machine Drive System," in Proceedings of Australasian Universities Power Engineering Conference- AUPEC'01, Perth, Australia, pp281-286, 2001
- [39] Mircea Popescu "Induction motor modelling for vector control purposes", Helsinki University of technology, laboratory of electromechanics, espoo 2000, 144 p.
- [40] Alfiedo Nava-Segura, Carlos Hembdez-Arhuburo, Gerard0 Mino-Aguilar.CIEP "Instantaneous Space Vector Model for Direct Flux and Torque Control of an Inverter Controlled Induction Motor" VII IEEE International Power Electronics Congress, CIEP, Oct 2000, pp.35-41.
- [41] C. Mademli & N. Margaris "Loss minimization in vector-controlled interior permanent-magnet synchronous motor drives", IEEE Transactions on Industrial Electronics, Aug 2002, Vol 49 , Issue: 6, pp 1344 - 1347 .
- [42] Y. Takeda S. Morimoto, Y. Tong & T. Hirasu "Loss minimization control of permanent magnet synchronous motor drives", IEEE Transactions on Industrial Electronics , Dec 1994 , Vol 41 , Issue: 5, pp 511 - 517.
- [43] H. Wijenayake & P. B. Schmidt. "Modeling and analysis of permanent magnet synchronous motor by taking saturation and core loss into account" Power Electronics and Drive Systems, 1997.Proceedings., 1997 International Conference, pp 530 – 534 vol.2 .
- [44] Ahmad Faiz Noor Azam, Auzani Jidin, Nor Azazi Ngatiman, M.H Jopri, Mustafa Manap, Adeline Lukar Herlino, Nor Faezah Alias "Current Control of BLDC Drives for EV Application" IEEE 7th International Power Engineering and Optimization Conference (PEOCO2013), June 2013 ,pp3-4.
- [45] QI Peng "An Improved Pso-Based Optimum Design of

Speed Controller for BLDC Motor” International Conference on Automatic Control and Artificial Intelligence ACAI March 2012, pp.453-456.

- [46] Muhammad Salman Khan “Development Of Detailed Drive Model In Matlab/Simulink With Automatic Optimization Of Control Loops” Master of Science Space Engineering - Space Master Luleå University of Technology Department of Computer Science, Electrical and Space Engineering 2012.
- [47] Emil klintberg “Comparison of Control Approaches for Permanent Magnet Motors” Master of Science Thesis Department of Energy and Environment Division of Electric Power Engineering, CHALMERS UNIVERSITY OF TECHNOLOGY Göteborg, Sweden 2013.
- [48] K. R. Rajagopal , Ajay Nair “Design and Development of a TMS320F2812 DSP Controller Based PM BLDC Motor Drive”, International Conference on Electrical Machines and Systems (ICEMS), Oct 2010, pp. 776-780.
- [49] S.S.Bharatkar, D.Chatterjee, A.K.Ganguli “Comparison of Switching Schemes for Brushless DC Motor Drives”, International Conference on Electrical Engineering/Electronics, Computer, Telecommunications and Information Technology, ECTI-CON, May 2010.
- [50] Sergio Andrés Reyes Sierra, Jorge Francisco, Martínez Carballido, José Luis Vázquez González, “Switching Techniques for Brushless DC Motors” International Conference on Electronics, Communications and Computing (CONIELECOMP), March 2013 ,pp. 162 – 166.
- [51] R. Shanmugasundram, K. Muhammad Zakariah, and N. Yadaiah, “Implementation and Performance Analysis of Digital Controllers for Brushless DC Motor Drives” IEEE/ASME Transactions on Mechatronics, Vol. 19, No. 1, Feb 2014.
- [52] Nicola Bianchi. “Analysis and Design of a PM Brushless Motor for High-Speed Operations”, IEEE Transactions on energy conversion , Sept 2000, vol. 20, no. 3.